

Probing the structural features that influence the mesomorphic properties of substituted dibenz[*a,c*]anthracenes

Joseph A. Paquette, Katie M. Psutka, Colin J. Yardley, and Kenneth E. Maly

Abstract: We report the synthesis and mesophase characterization of a series of novel hexaalkoxydibenzanthracenes to probe the effect of side-chain length variation and substituents on the mesophase temperature range. A series of hexaalkoxydibenz[*a,c*]anthracenes (**2a–2i**) with varying chain lengths were prepared by Suzuki coupling of the appropriate boronate ester with the corresponding dialkoxydibromonaphthalenes, followed by oxidative cyclization. Compounds **2a–2i** were also brominated in the 10 and 13 positions to yield the corresponding dibromo series, **4a–4i**. While none of the compounds, **2a–2i**, exhibited columnar mesophases, all of the compounds in series **4a–4i** did exhibit columnar phases over broad temperature ranges. To further investigate the effect of substituents on the mesomorphic properties of hexaalkoxydibenzanthracenes, we also prepared iodo-substituted **8**, nitro-substituted **9**, and amino-substituted **10**. A comparison of the mesophase temperature range with previously reported compounds **3–7** shows that electron-withdrawing groups promote the formation of stable mesophases. However, our results also suggest that the substituents affect mesophase stability by participating in intermolecular contacts within the columnar stacks of the mesophase.

Key words: liquid crystals, aromatic compounds, self-assembly, π – π interactions, synthesis.

Résumé : Nous présentons la synthèse et la caractérisation en mésophase d'une série de nouveaux hexaalkoxydibenzanthracènes afin d'explorer l'effet de variation de la longueur des chaînes latérales et de la nature des substituants sur l'intervalle de températures de la mésophase. Nous avons synthétisé une série d'hexaalkoxydibenz[*a,c*]anthracènes (**2a–2i**), dont la longueur des chaînes latérales variait, au moyen d'un couplage de Suzuki entre les esters boroniques appropriés et les dialcoxydibromonaphthalènes correspondants, suivi d'une cyclisation oxydante. Nous avons également soumis les composés **2a–2i** à une bromination aux positions 10 et 13 pour produire la série de dibromures correspondants **4a–4i**. Alors qu'aucun des composés **2a–2i** n'a présenté de mésophases colonnaires, tous les composés de la série **4a–4i** ont présenté des phases colonnaires dans un large intervalle de températures. Afin d'approfondir l'étude des effets des substituants sur les propriétés mésomorphiques des hexaalkoxydibenzanthracènes, nous avons également préparé les dérivés iodo **8**, nitro **9** et amino **10**. Une comparaison des intervalles de températures de la mésophase avec ceux des composés **3–7** publiés antérieurement a permis de montrer que les groupes électroattracteurs favorisent la formation de mésophases stables. Cependant, nos résultats laissent également supposer que les substituants ont une influence sur la stabilité des mésophases à cause de leur participation aux contacts intermoléculaires dans les empilements colonnaires de la mésophase. [Traduit par la Rédaction]

Mots-clés : cristaux liquides, composés aromatiques, auto-assemblage, interactions pi, synthèse.

Introduction

Columnar liquid crystalline phases are formed from disc-shaped compounds that typically feature a polycyclic aromatic core with several peripheral flexible side chains.^{1–3} In the columnar liquid crystal phase (mesophase), these compounds form π -stacked arrays that allow them to transport charge along the columnar axis. Because of their charge transport properties, these materials show promise as organic semiconductors that can be used in applications such as photovoltaic solar cells, organic light emitting diodes, and field effect transistors.^{4–6} A key requirement for the use of these materials as organic semiconductors is the ability to tune the liquid crystal phase range to suit the desired application. Therefore, understanding how molecular structure influences the mesomorphic properties is critically important for the design of these materials.

Columnar mesophases arise in part from a microsegregation of the aromatic cores, which promote crystalline order, from the side chains, which are liquid-like and flexible.¹ As such, the nature and length of the side chains are very important factors in determining the mesophase temperature range. However, given that columnar mesophases have significant π – π stacking within the columns, noncovalent interactions such as π stacking are thought to play an important role in mesophase formation and in determining the stability of the mesophase. Consequently, the structure and size of the aromatic core are important determining factors in controlling the mesophase temperature range, with larger aromatic cores often showing broad mesophase ranges with high clearing temperatures.^{7–12} The introduction of substituents onto the aromatic core can impact the extent of π -stacking interactions and therefore be used to tune mesophase stability.^{13–15}

Received 21 September 2016. Accepted 24 October 2016.

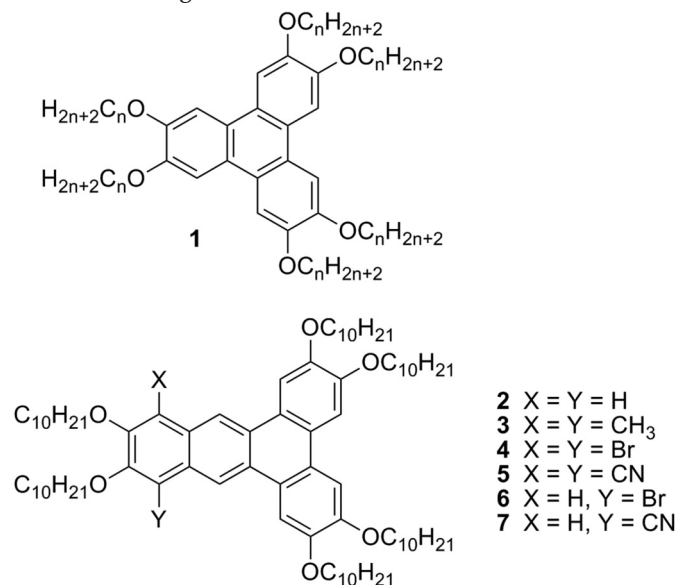
J.A. Paquette, K.M. Psutka, C.J. Yardley, and K.E. Maly. Department of Chemistry and Biochemistry, Wilfrid Laurier University, Waterloo, ON N2L 3C5, Canada.

Corresponding author: Kenneth E. Maly (email: kmaly@wlu.ca).

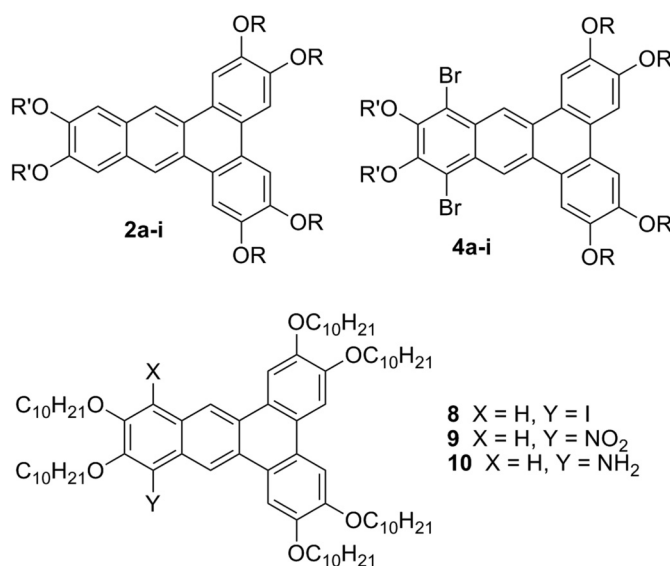
This paper is part of a Special issue to honor Professor Reginald Mitchell.

Copyright remains with the author(s) or their institution(s). Permission for reuse (free in most cases) can be obtained from RightsLink.

Hexaalkoxytriphenylenes such as **1** are among the most widely studied columnar liquid crystalline materials, although they typically exhibit columnar mesophases over relatively narrow temperature ranges above room temperature.^{16–18} Alkoxy-substituted dibenz[*a,c*]anthracenes (e.g., **2–7**), where the polycyclic aromatic hydrocarbon (PAH) core is extended as compared to the corresponding triphenylenes, have until recently received relatively little attention as potential columnar liquid crystalline materials.^{11,19–21} Williams and co-workers¹¹ were the first to report an example of a dibenzanthracene derivative (**3**) exhibiting a columnar hexagonal mesophase. The mesophase range of **3** was much broader than that of the corresponding triphenylene, suggesting that extending the aromatic core stabilizes the mesophase through improved π -stacking interactions. More recently, we reported the synthesis and mesophase characterization of a series of related hexa-(decyloxy)dibenz[*a,c*]anthracenes (**2**, **4–7**).¹⁹ Surprisingly, the parent hexa(decyloxy)dibenz[*a,c*]anthracene (**2**) did not exhibit any columnar liquid crystalline phase, while compounds **3–7**, bearing substituents in the 10 and (or) 13 positions all exhibited columnar mesophases over broad temperature ranges. Based on this limited set of dibenzanthracene derivatives, electron-withdrawing substituents in these positions appear to promote the formation of stable mesophases over broad temperature ranges. These results are consistent with other reports that show electron-withdrawing substituents attached to the disc-shaped core lead to the formation of mesophases over broad temperature ranges.^{13,15} Together, these studies support the idea that electron-withdrawing groups pull electron density away from the aromatic core and thereby favour π stacking.^{13,22,23}



However, the absence of a mesophase for the parent compound **2** as compared with **3**, which bears electron-donating methyl groups, suggests that other factors are influencing the mesophase behaviour, and that substituents are not simply exerting an electronic effect, which has also been noted with triphenylene derivatives.²⁴ To further explore how structural features influence liquid crystalline properties in this class of compounds, we report an expanded study that examines the effect of chain length variation on the mesophase temperature range of dibenzanthracenes **2a–2i** and their brominated derivatives **4a–4i**. We have also prepared an expanded set of dibenzanthracenes (**8–10**) bearing substituents at the 10 or 10 and 13 positions to investigate the effect of substituents on the aromatic core on columnar liquid crystalline properties.



Results and discussion

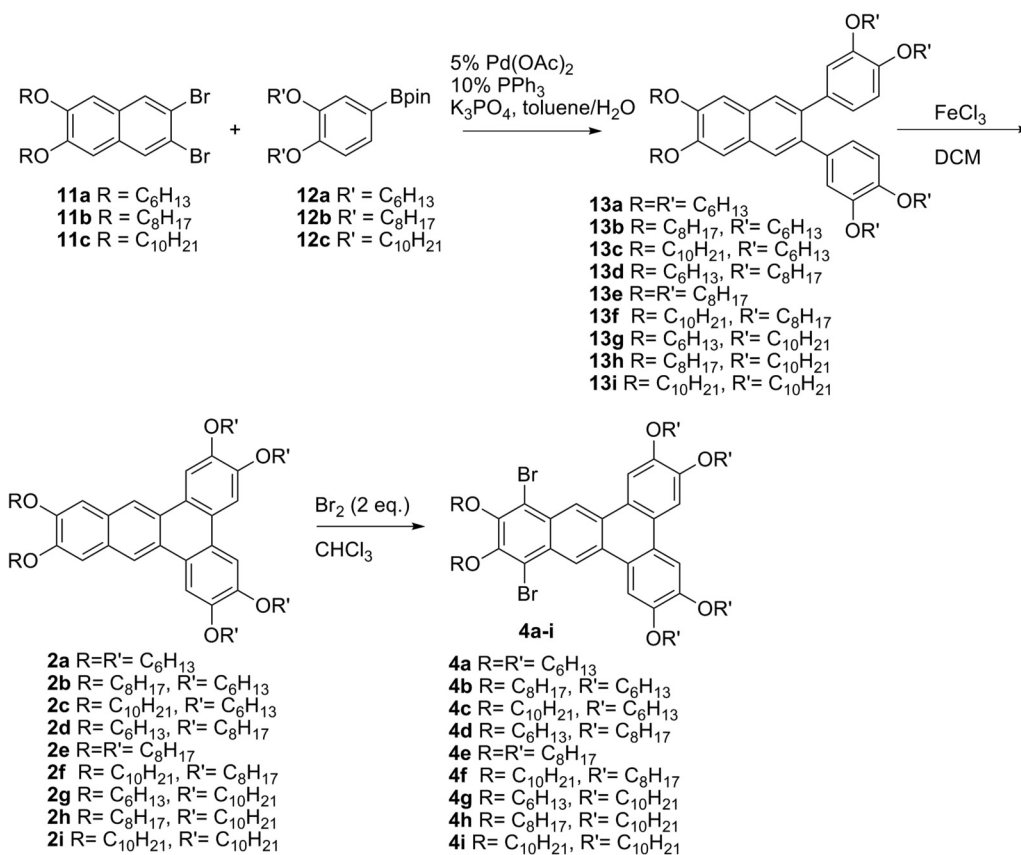
Synthesis

We previously reported the synthesis of hexa(decyloxy)dibenz[*a,c*]anthracene (**2**) using an approach involving a Suzuki–Miyaura cross coupling of a substituted naphthalene and an alkoxy-substituted aryl boronate, followed by an oxidative cyclization.¹⁹ We also demonstrated that electrophilic bromination introduced substituents in the 10 and 13 positions. By careful control of the stoichiometry of bromine added, either the monobromo derivative **6** or the dibromo derivative **4** could be formed. Here, we employed a similar approach to prepare a series of hexaalkoxydibenz[*a,c*]anthracenes and their dibromo-substituted derivatives where the alkoxy chain lengths were varied from hexyl to decyl chains. It is noteworthy that with this modular approach we can independently vary the side chains on the anthracene moiety and the fused benzene rings, allowing us to produce a set of nine compounds from the three different chain lengths. The appropriate 2,3-dialkoxy-6,7-dibromonaphthalene^{19,25,26} (**11a–11c**) and dialkoxyphenyl boronate ester (**12a–12c**)¹⁹ underwent Suzuki cross coupling to yield compounds **13a–13i** (Scheme 1). While the Suzuki couplings gave the desired diaryl naphthalenes in moderate to good yields, purification of these compounds proved challenging: in many cases side-products remained after column chromatography and these relatively low-melting solids were difficult to purify by recrystallization. Therefore, these compounds were used without further purification in the subsequent oxidative cyclizations. The oxidative ring closing furnished the desired hexaalkoxydibenzanthracenes (**2a–2i**), which were readily purified by column chromatography and recrystallization. Bromination using Br₂ in CHCl₃ yielded the corresponding dibromo derivatives **4a–4i**.

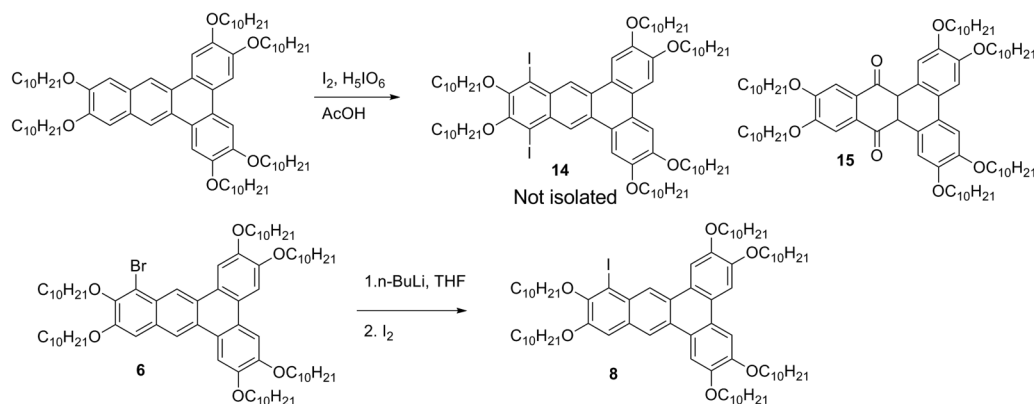
Given that the introduction of bromo substituents in the 10 and 13 positions proceeded well, we decided to use electrophilic aromatic substitutions to introduce other substituents onto the hexadecyloxydibenzanthracene **2i** to probe the effects of these substituents on mesomorphic properties. Unfortunately, efforts to prepare the corresponding mono- and di-iodo-substituted dibenzanthracene derivatives **8** and **14** using standard iodination conditions of iodine in periodic acid in glacial acetic acid were unsuccessful, leading instead to the oxidation of **2i** to give the corresponding dibenzanthracenequinone **15** (Scheme 2). To circumvent this problem, the monoiodo derivative **8** was prepared in a 51% yield by lithium–halogen exchange of compound **6** and subsequent trapping with iodine.

Direct nitration of **2** was also unsuccessful, possibly because of the limited solubility of the starting material in the reaction

Scheme 1.



Scheme 2.



conditions. We therefore carried out nitration on the dibromodicyloxynaphthalene (**11c**) to give compound **16** in a 55% yield, which was then subjected to Suzuki cross coupling with the aryl boronate **12c** to furnish **17** in a 59% yield (Scheme 3). Subsequent oxidative cyclization yielded the desired nitro-substituted compound **9** in a 91% yield. The nitro compound **9** could be used to access the corresponding amino derivative (**10**). After attempting several different standard reduction methods for converting aromatic nitro compounds to the corresponding anilines, we found that sodium borohydride in the presence of nickel chloride hexahydrate in tetrahydrofuran (THF)/methanol furnished **12** in a modest 24% yield.²⁷

Mesomorphic properties – effect of side chain variation

The mesomorphic properties of compounds **2a–2i** and **4a–4i** were evaluated by polarized optical microscopy and differential

scanning calorimetry (DSC). The phase transition temperatures of these compounds are summarized in Fig. 1. None of the parent hexaalkoxydibenzanthracene derivatives (**2a–2i**) exhibited columnar mesophases, instead showing transitions directly from the crystalline solid to isotropic liquid. The melting points of **2a–2i** ranged from approximately 60–90 °C, with those compounds with longer alkoxy chains having lower melting points. The distinct absence of any columnar mesophases for series **2a–2i** is surprising, especially since all of the corresponding triphenylene derivatives (**1**) exhibit columnar hexagonal phases.^{28,29} The reasons for these differences are not clear, but may be the result of differences in effective packing: in the columnar phase, the triphenylenes can pack effectively in a columnar stack, while the slightly elongated dibenzanthracenes do not pack as well in the columns.

Scheme 3.

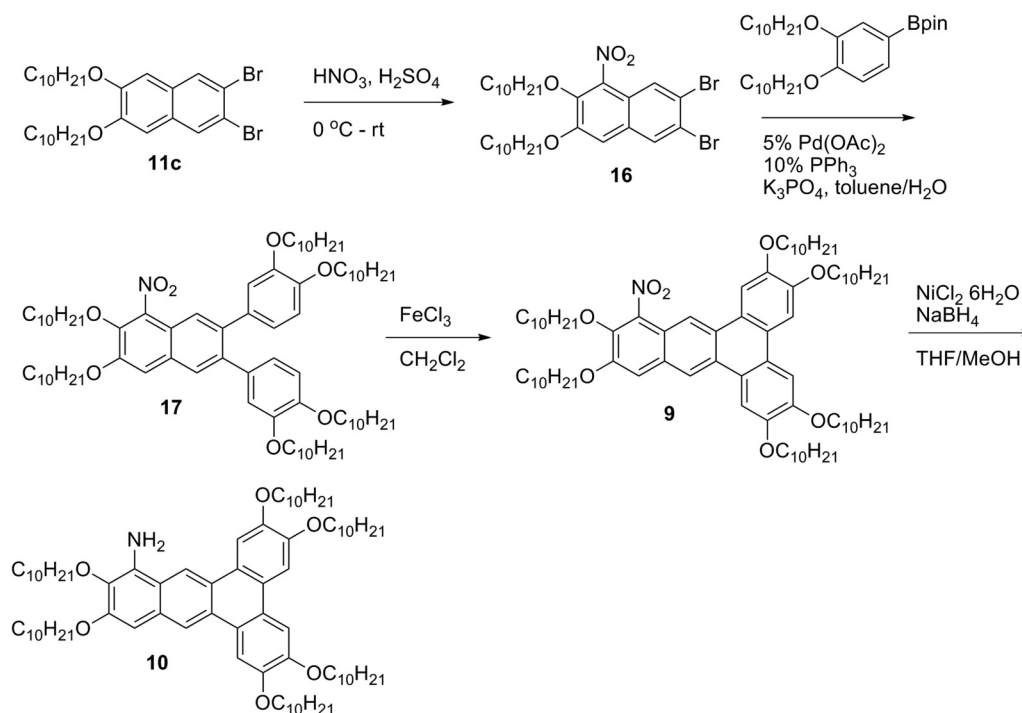
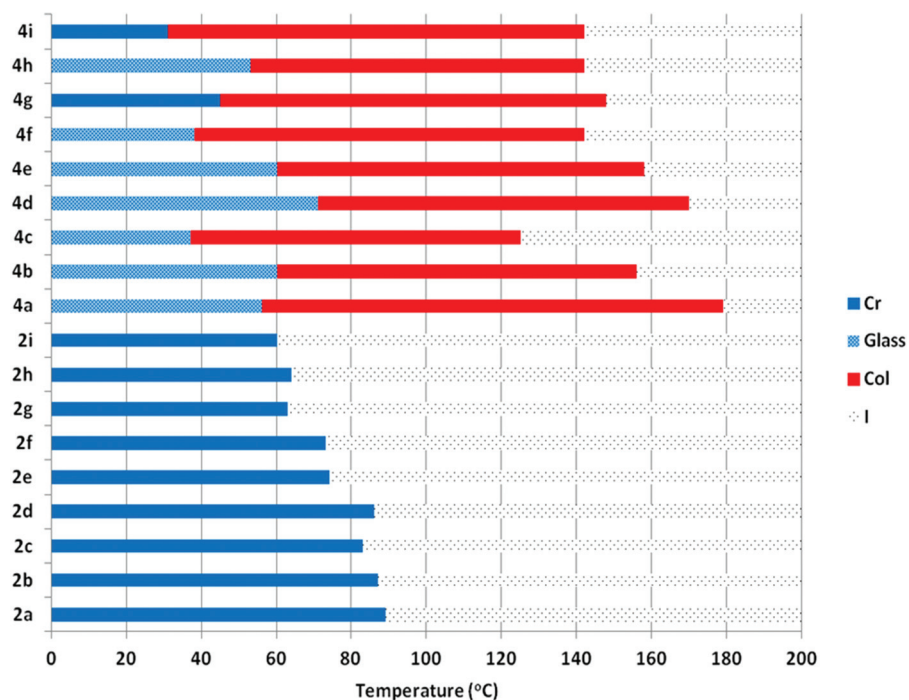


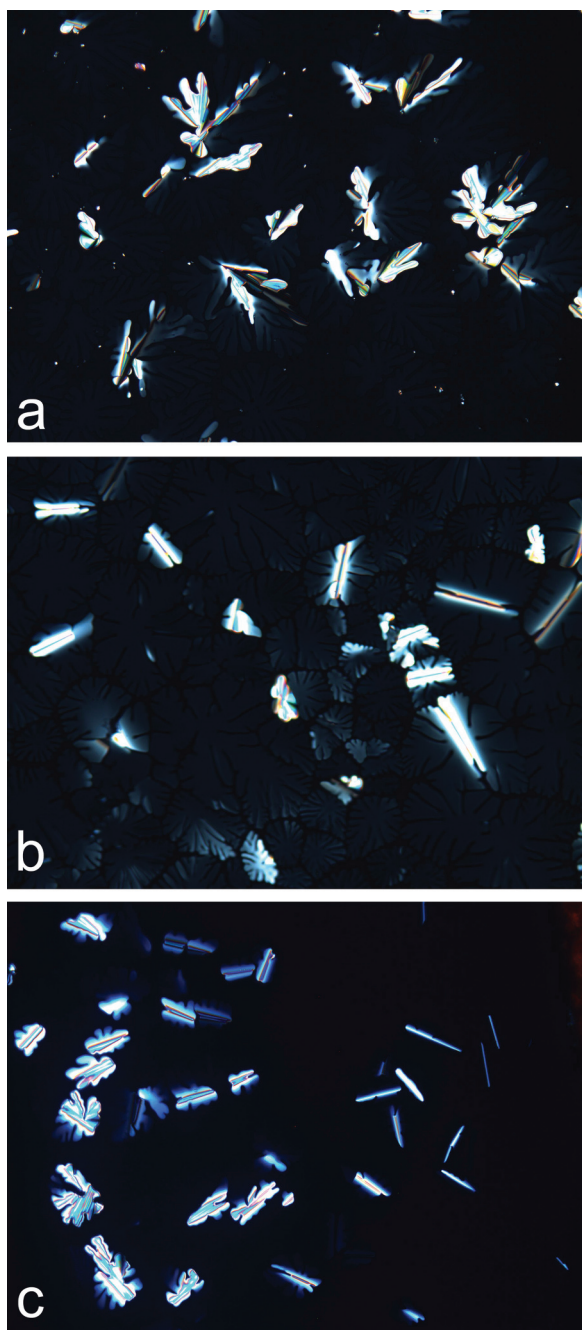
Fig. 1. Summary of phase transition temperatures for compounds **2a–2i** and **4a–4i** determined by differential scanning calorimetry (DSC) on the 2nd heating. The glass–mesophase transitions were not always clearly observed by DSC, so polarized optical microscopy was used in these cases.



Similarly, hexaalkoxydibenzophenazines, which are structurally very similar to the dibenzanthracenes, exhibit columnar mesophases over broad temperature ranges. The difference in mesomorphic behaviour between the dibenzanthracenes and the corresponding dibenzophenazines may be attributed to differences in the propensity of these compounds to engage in π -stacking interactions. The electron-deficient heteroaromatic dibenzophenazine is more likely to form π stacks than the electron-rich dibenzanthracene.^{19,30}

In contrast to the hexaalkoxydibenzanthracene series **2a–2i**, all of the dibromo-substituted compounds (**4a–4i**) exhibit columnar mesophases over broad temperature ranges (Fig. 1). Polarized optical microscopy of compounds **4a–4i** showed dendritic textures with homeotropically aligned domains consistent with uniaxial columnar hexagonal phases (Fig. 2). Variable-temperature powder X-ray diffraction (XRD) studies on a representative compound in this series supports the phase assignment as a columnar hexagonal mesophase.¹⁹ It is noteworthy that most of the compounds in

Fig. 2. Representative polarized optical micrographs of (a) **4b**, (b) **4g**, and (c) **4e** taken upon cooling near the isotropic liquid–columnar mesophase transition.



series **4** do not crystallize on cooling from the columnar mesophase but instead form glasses that preserve the order of the columnar mesophase. In some cases, these glass transitions could be distinguished by DSC, while in other cases they were determined by polarized optical microscopy as the point at which the textures no longer change upon shearing or compression.

The stability of the mesophase is reflected by the clearing point (the transition between the liquid crystal phase and isotropic liquid phase), with a higher clearing point corresponding to a more stable mesophase. As such, even though the melting transition is not clearly observed because of the formation of a glassy phase, the mesophase characteristics in this series of compounds can be compared by considering the clearing points, which are clearly

observable by polarized optical microscopy and differential scanning calorimetry. A comparison of the clearing points of compounds **4a** ($R = R' = C_6$), **4e** ($R = R' = C_8$), and **4i** ($R = R' = C_{10}$) reveals that shorter side chains lead to increased clearing points.

When the side chains on the benzo-fused rings is $R = C_{10}H_{21}$, changing the R' side chains adjacent to the bromo substituents from hexyl to decyl has only a small effect on the clearing point. In contrast, when $R = C_6H_{13}$, changing the R' substituent has a more dramatic effect on the clearing point, with shorter R' chains leading to higher clearing points. Thus, the effect of the R and R' side chains on the mesophase range is interrelated. The interdependence of both side chains on the fused benzene rings and the anthracene moieties may be due to overall changes in molecular shape from more disc shaped to elliptical. For example, compound **2c**, bearing hexyloxy chains on the fused benzo groups and decyloxy chains on the anthracene end, has the lowest clearing point and is also the compound with the most elongated, elliptical shape.

Overall, the observation of columnar mesophases over broad temperature ranges for series **4a–4i** while series **2a–2i** shows no mesomorphic behaviour suggests that the bromo substituents in the 10 and 13 positions of **4a–4i** are important for the formation of columnar mesophases in these systems and lead to the formation of very stable mesophases. A possible explanation for the induction of stable mesophases upon bromination is that the bromine atoms increase the surface area of the core of the molecule, thereby increasing van der Waals interactions in the columnar stacks.³¹ The increased intermolecular contacts involving the bromo substituents would also be expected in the solid state, and should give rise to an increase in the melting transition temperature. However, as already noted, compounds **4a–4i** have mesophases extending to relatively low temperatures and generally do not solidify upon cooling; instead, they exhibit glassy states at low temperature. This behaviour can be attributed to the bromo groups influencing the conformational distribution of the adjacent alkoxy side chains. In **4a–4i**, these side chains are not coplanar with the aromatic ring, which may prevent effective packing in the crystalline solid.

To further probe the effect of substituents on the aromatic core on mesomorphic properties, we examined the effect varying substituents in the 10 or 10 and 13 positions of the hexaalkoxydibenzanthracenes while maintaining a constant side-chain length. Specifically, we compared the mesomorphic behaviour of compounds **3–7**, which had been previously reported,^{11,19} to compounds **8–10**, which were prepared in this study.

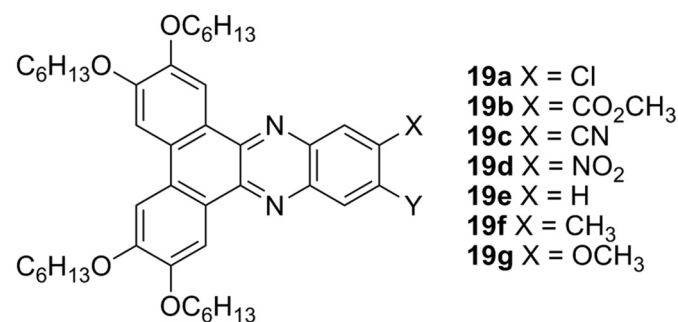
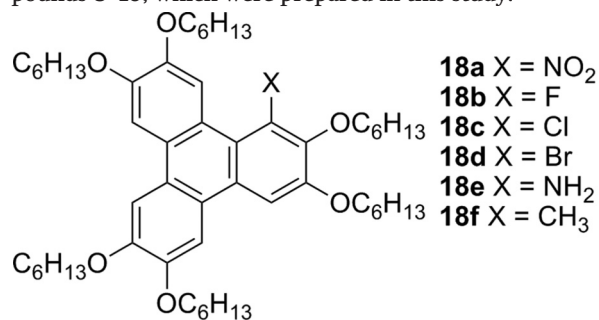
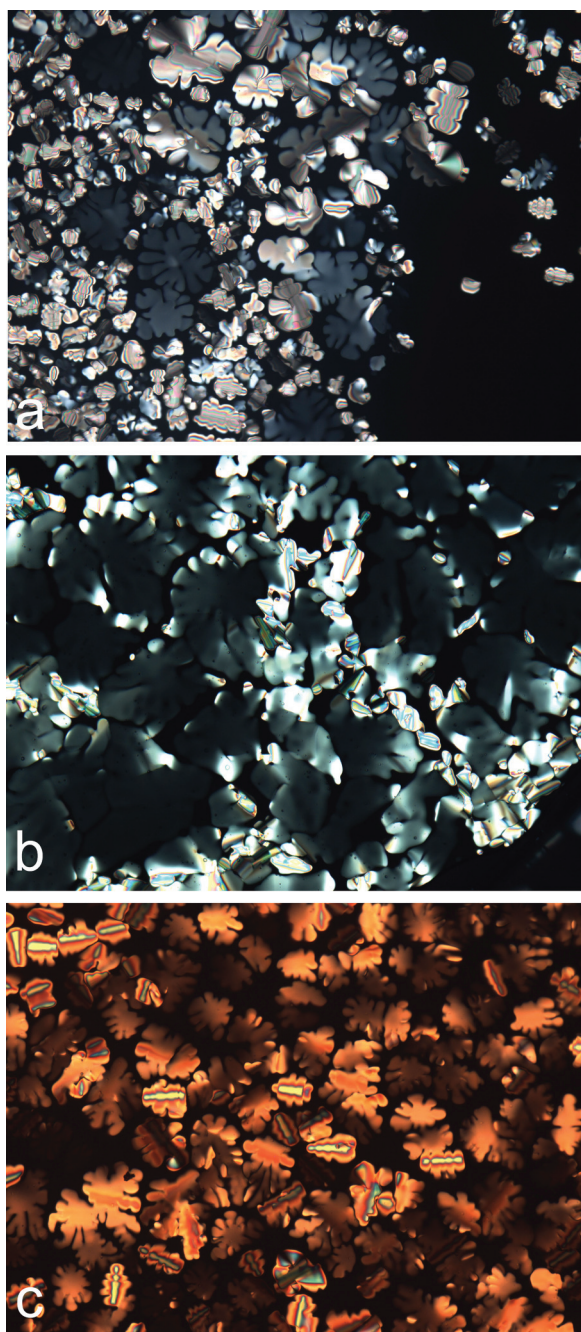


Fig. 3. Representative polarized optical micrographs of compounds (a) **8**, (b) **9**, and (c) **10** near the isotropic–columnar phase transition, upon cooling.



All of the compounds bearing substituents in the 10 or 10 and 13 positions exhibited columnar mesophases as shown by DSC and polarized optical microscopy (Table 1). Furthermore, polarized optical microscopy studies (Fig. 3) as well as variable-temperature powder XRD on a subset of these compounds¹⁹ show that these compounds form columnar hexagonal mesophases.

Several studies have suggested that electron-withdrawing substituents attached to the aromatic core of a discotic mesogen lead to broad mesophase temperature ranges with increased clearing points.^{13–15,32,33} For example, Bushby and co-workers^{14,15,32} showed that the addition of substituents onto the core of a hexaalkoxytriphenylene significantly influences the mesophase temperature range (**18a–18f**). Specifically, strong electron-withdrawing

Table 1. Summary of phase transition temperatures of **4–10**.

Compound	X, Y	Transition temperature (°C) ^a
4 ¹⁹	X = Y = Br	Cr 31 Col 142 I
5 ¹⁹	X = Y = CN	Cr -16 G 25 Col 243 I
6 ¹⁹	X = Br, Y = H	Cr 61 Col 113 I
7 ¹⁹	X = CN, Y = H	Cr 51 Col 193 I
8	X = I, Y = H	Cr 62 Col 109 I
9	X = NO ₂ , Y = H	Cr 46 Col 170 I
10	X = NH ₂ , Y = H	Cr 34 Col 86 I

^aPhase transition temperatures are reported by DSC upon heating at 5 °C/min and are reproducible over three heating and cooling cycles. Col = columnar, Cr = crystal, G = glassy, I = isotropic.

substituents such as nitro and fluoro groups lead to higher clearing transition temperatures, while electron-donating methyl or amino groups showed a significant lowering of the clearing point or even a disappearance of the mesophase. Similarly, Williams and co-workers¹³ demonstrated that the mesophase stability as estimated from the clearing transition temperature showed a good correlation with Hammett σ values in a series of substituted dibenzophenazines (**19a–19f**). For compounds **19e–19g**, bearing electron-withdrawing groups, no mesophase was observed.¹³

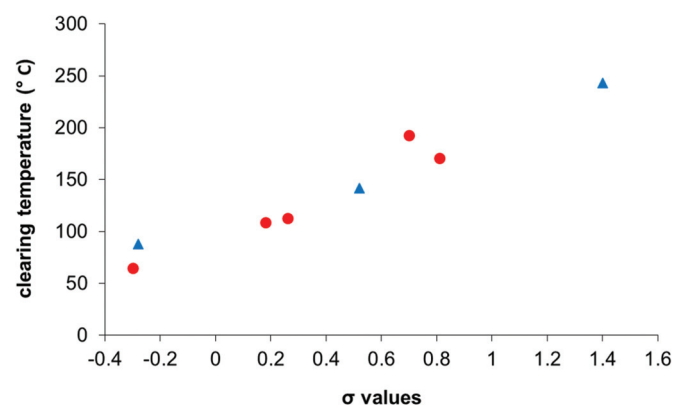
The higher clearing points associated with stabilization of the mesophase can be attributed to more favorable π -stacking interactions.¹³ In electron-rich aromatic systems such as alkoxy-substituted triphenylenes, π -stacking interactions are electrostatically disfavoured between two electron-rich aromatic systems. The addition of electron-withdrawing substituents reduces the electron density of the aromatic ring; consequently, the repulsive interactions are minimized, thereby stabilizing the mesophase.^{13,22,23} It is noteworthy that in many of these systems the electron-withdrawing groups also introduce a dipole moment, so the mesophase may be further stabilized by dipole–dipole interactions.

To probe the potential electronic effects of substituents on the mesophase temperature in our hexaalkoxydibenzanthracenes, we made a similar comparison of clearing transition temperatures with Hammett parameters (σ_p). The plot of clearing point versus Hammett σ_p for both the monosubstituted series and disubstituted series shows a strong correlation ($R^2 = 0.95$) (Fig. 4), consistent with previous findings that suggest that electron-withdrawing substituents stabilize the mesophase.

However, the absence of any columnar mesophase for the parent hexaalkoxydibenzanthracene (**2**) is a notable exception to this trend. The absence of a mesophase for **2** even though compounds **3**¹¹ and **10** (which are more electron rich) do exhibit columnar mesophases, suggests that the substituents on the dibenzanthracene core are not stabilizing the mesophase purely by electronic effects. This behaviour is in contrast with the corresponding hexaalkoxytriphenylenes, where compounds **18e** and **18f**, bearing amino and methyl groups, respectively, do not exhibit mesophases, while the parent hexaalkoxytriphenylene does. We propose that the compounds bearing substituents in the 10 or 10 and 13 positions are able to pack more effectively in the columnar mesophase with more extensive intermolecular contacts. In other words, the parent dibenzanthracene (**2**), with its elongated polycyclic core, could stack into columns but would leave void spaces due to inefficient packing. By placing substituents on the core, the core becomes more disc shaped and can pack more effectively by involving the substituents in the intermolecular contacts within the columnar stacks.

Support for the proposed increased surface for intermolecular stacking interactions with substituents is provided by the comparison of compounds **2a–2i** and their dibrominated derivatives

Fig. 4. Clearing transition temperature vs Hammett σ_p values. The red circles correspond to the monosubstituted series (6, 7, 8–10), while the blue triangles correspond to the disubstituted series (3, 4, 5). For disubstituted compounds 3–5, the Hammett σ_p values were doubled to account for the two substituents.



4a–4i (Fig. 1). While none of compounds **2a–2i** exhibit columnar mesophases, all of compounds **4a–4i** exhibit columnar mesophases with high clearing points, in most cases close to 100 °C higher than the melting points of **2a–2i**. It is plausible that the observed differences between these two series are the result of improved intermolecular interactions within the columns as opposed to an electronic effect of relatively weakly electron-withdrawing bromo substituents.

Conclusions

In summary, we have prepared a series of hexaalkoxydibenzanthracenes with varying alkoxy side chains and their bromo derivatives. The hexaalkoxydibenzanthracenes do not exhibit columnar mesophases, regardless of the side-chain lengths. In contrast, the bromo-substituted derivatives all exhibit columnar mesophases over broad temperatures ranges. We have also prepared a series of hexaalkoxydibenzanthracene derivatives where the substituents on the core are varied to probe the effect of substituents on the mesophase temperature range. Our results suggest that electronic effects of substituents on the core influence the mesophase range, with electron-withdrawing substituents stabilizing the mesophase. However, our results also indicate that the substituent effects on the mesophase range are also influenced by other factors. Specifically, we propose that substituents are able to participate in intermolecular contacts within the columns, effectively increasing the size of the core and promoting the formation of extended π -stacked arrays.

Experimental

Synthesis

^1H and ^{13}C nuclear magnetic resonance (NMR) spectra were recorded using a Varian 300 MHz Unity Inova NMR spectrometer, using indicated deuterated solvents purchased from Cambridge Isotope Laboratories, Inc. (CIL). All chemicals used were purchased from Sigma-Aldrich and were used as received. 1-Pinacolatoboron-3,4-bis(alkoxy)benzenes (**12a–12c**)¹⁹ and 2,3-dibromo-6,7-dialkoxynaphthalenes (**11a–11c**)^{19,25,26} were prepared according to literature procedures. Compounds **2i**, **4i**, and **5–7** were reported previously.¹⁹ Anhydrous and oxygen-free solvents were dispensed from a custom-built solvent purification system that used purification columns packed with activated alumina and supported copper catalyst (Glasscontour, Irvine, CA). Oven- or flame-dried glassware was used for all reactions. Melting points were determined by DSC at a heating rate of 5 °C/min and are reported from the peak of the phase transition. High resolution matrix-assisted laser desorption ionization (MALDI) mass spectra were recorded at

the Centre Régional de Spectrométrie de Masse à l'Université de Montréal using an Agilent LC/MSD TOF spectrometer.

General procedure for the synthesis 1,2-dialkoxy-5,6-bis(3,4-dialkoxybenzene)naphthalene (**13**)

$\text{Pd}(\text{OAc})_2$ (5%) and PPh_3 (10%) were dissolved in 20 mL degassed toluene, followed by the addition of 2,3-dibromo-6,7-bis(decyloxy)naphthalene (1 equiv.) and 1-pinacolatoboron-3,4-bis(decyloxy)benzene (2.09 equiv.). To the reaction mixture 7 mL of degassed aqueous 2.0 mol/L K_3PO_4 (excess) was added. The mixture was heated to 80 °C and left to stir for 48 h. The reaction mixture was cooled to room temperature, followed by the addition of 20 mL dichloromethane (DCM) and washed with H_2O (2 × 20 mL) and brine (1 × 20 mL). The organic layer was dried with MgSO_4 and the solvent removed under reduced pressure to give the product. The crude product was further purified using column chromatography with hexanes/dichloromethane (60:40) unless otherwise stated. Due to difficulties with purification, compound series **13** was used without further purification.

General procedure for the synthesis of hexaalkoxydibenz[a,c]anthracenes (**2a–2i**)

2,3-Bis[3,4-dialkoxyphenyl]-6,7-dialkoxynaphthalene (1 equiv.) was dissolved in 20 mL dry CH_2Cl_2 . FeCl_3 (6 equiv.) was added to the solution and stirred for 1 h. The solution was poured into MeOH (100 mL) and the resulting precipitate was collected by suction filtration. The crude product was purified by a short silica column eluting with CH_2Cl_2 and the solvent was removed via rotary evaporator, followed by recrystallization in acetone.

2,3,6,7,11,12-Hexakis(hexyloxy)dibenz[a,c]anthracene (**2a**)

2,3-Bis[3,4-dihexyloxybenzene]-6,7-bis(hexyloxy)naphthalene (0.214 g, 0.243 mmol) and FeCl_3 (0.241 g, 1.48 mmol) were used, which yielded a light brown solid (0.136 g, 64%); mp 89 °C. ^1H NMR (300 MHz, CDCl_3) δ : 8.70 (s, 2H), 8.11 (s, 2H), 7.81 (s, 2H), 7.33 (s, 2H), 4.31–4.18 (m, 12H), 2.00–1.93 (m, 12H), 1.61–1.55 (m, 12H), 1.47–1.39 (m, 24H), 0.98–0.92 (18H). ^{13}C NMR (75 MHz, CDCl_3) δ : 150.08, 149.50, 149.28, 128.31, 126.71, 124.28, 124.14, 119.57, 107.93, 107.70, 107.02, 70.02, 69.63, 69.07, 31.93, 31.87, 29.68, 29.65, 29.33, 26.11, 26.08, 22.92, 22.89, 14.32, 14.30. HRMS (MALDI) calcd. for $\text{C}_{58}\text{H}_{86}\text{O}_6$ m/z : 878.6424; found: 878.6419.

2,3,6,7-Tetrakis(hexyloxy)-11,12-bis(octyloxy)dibenz[a,c]anthracene (**2b**)

2,3-Bis[3,4-dihexyloxyphenyl]-6,7-dioctyloxynaphthalene (0.20 g, 0.214 mmol) and FeCl_3 (0.212 g, 1.304 mmol) were used to obtain a light brown solid (0.19 g, 94.9% yield); mp 87 °C. ^1H NMR (300 MHz, CDCl_3) δ : 8.71 (s, 2H), 8.12 (s, 2H), 7.81 (s, 2H), 7.33 (s, 2H), 4.32–4.18 (m, 12H), 2.00–1.93 (m, 12H), 1.62–1.55 (m, 12H), 1.43–1.32 (m, 32H), 0.98–0.91 (m, 18H). ^{13}C NMR (75 MHz, CDCl_3) δ : 149.41, 148.83, 148.60, 127.63, 126.02, 123.60, 123.47, 118.86, 107.05, 106.36, 69.34, 68.96, 68.39, 31.39, 31.23, 28.95, 28.84, 28.67, 25.68, 25.38, 25.01, 22.20, 13.65, 13.59. HRMS (MALDI) calcd. for $\text{C}_{62}\text{H}_{94}\text{O}_6$ m/z : 934.7050; found: 934.7033.

2,3,6,7-Tetrakis(hexyloxy)-11,12-bis(decyloxy)dibenz[a,c]anthracene (**2c**)

2,3-Bis[3,4-dihexyloxyphenyl]-6,7-didecyloxynaphthalene (0.75 g, 0.75 mmol) and FeCl_3 (0.737 g, 4.53 mmol) were used to obtain a light brown product (0.70 g, 94% yield); mp 83 °C. ^1H NMR (300 MHz, CDCl_3) δ : 8.70 (s, 2H), 8.11 (s, 2H), 7.80 (s, 2H), 7.32 (s, 2H), 4.31–4.17 (m, 12H), 1.97–1.92 (m, 12H), 1.61–1.56 (m, 12H), 1.42–1.38 (m, 40H), 0.97–0.91 (m, 18H). ^{13}C NMR (75 MHz, CDCl_3) δ : 150.10, 149.52, 149.29, 128.32, 126.71, 124.29, 124.16, 119.56, 107.97, 107.05, 70.03, 69.64, 69.08, 32.16, 31.93, 31.16, 29.90, 29.84, 29.71, 29.67, 29.65, 29.61, 29.38, 26.38, 26.10, 26.08, 25.00, 22.93, 22.91, 22.90, 14.35, 14.31, 14.29. HRMS (MALDI) calcd. for $\text{C}_{66}\text{H}_{102}\text{O}_6$ m/z : 990.7676; found: 990.7685.

2,3,6,7-Tetrakis(octyloxy)-11,12-bis(hexyloxy)dibenz[a,c]anthracene (2d)

2,3-Bis[3,4-dioctyloxyphenyl]-6,7-dihexyloxynaphthalene (0.20 g, 0.201 mmol) and FeCl₃ (0.19 g, 1.23 mmol) were used to give a light brown solid (0.15 g, 75.3% yield); mp 86 °C. ¹H (300 MHz, CDCl₃) δ: 8.68 (s, 2H), 8.10 (s, 2H), 7.80 (s, 2H), 7.32 (s, 2H), 4.31–4.18 (m, 12H), 2.00–1.93 (m, 12H), 1.61–1.57 (m, 12H), 1.43–1.33 (m, 40H), 0.97–0.89 (m, 18H). ¹³C NMR (75 MHz, CDCl₃) δ: 150.11, 149.55, 149.31, 128.33, 126.72, 124.32, 124.19, 119.55, 108.02, 107.83, 107.08, 70.06, 69.69, 69.08, 32.11, 31.88, 29.74, 29.58, 29.36, 26.45, 26.44, 26.06, 22.94, 22.88, 14.35, 14.27. HRMS (MALDI) calcd. for C₆₆H₁₀₂O₆ *m/z*: 990.7676; found: 990.7685.

2,3,6,7,11,12-Hexakis(octyloxy)dibenz[a,c]anthracene (2e)

2,3-Bis[3,4-dioctyloxyphenyl]-6,7-dioctyloxynaphthalene (0.574 g, 0.547 mmol) and FeCl₃ (0.541 g, 3.340 mmol) were used to give a light brown solid (0.521 g, 90.9% yield); mp 74 °C. ¹H (300 MHz, CDCl₃) δ: 8.69 (s, 2H), 8.11 (s, 2H), 7.80 (s, 2H), 7.32 (s, 2H), 4.30–4.18 (m, 12H), 1.97–1.92 (m, 12H), 1.60–1.57 (m, 12H), 1.42–1.32 (m, 48H), 0.92–0.88 (m, 18H). ¹³C NMR (75 MHz, CDCl₃) δ: 150.10, 149.52, 149.30, 128.32, 126.71, 142.30, 124.17, 119.56, 107.77, 107.05, 70.05, 69.67, 69.09, 32.16, 32.10, 29.90, 29.84, 29.73, 29.71, 29.61, 29.58, 29.34, 26.44, 26.39, 25.01, 25.00, 22.93, 14.35. HRMS (MALDI) calcd. for C₇₀H₁₁₀O₆ *m/z*: 1046.8302; found: 1046.8297.

2,3,6,7-Tetrakis(octyloxy)-11,12-bis(decyloxy)dibenz[a,c]anthracene (2f)

2,3-Bis[3,4-dioctyloxyphenyl]-6,7-didecyloxynaphthalene (0.648 g, 0.586 mmol) and FeCl₃ (0.580 g, 3.57 mmol) were used to give a pale brown solid (0.208 g, 32.2% yield); mp 74 °C. ¹H NMR (300 MHz, CDCl₃) δ: 8.69 (s, 2H), 8.11 (s, 2H), 7.80 (s, 2H), 7.32 (s, 2H), 4.30–4.17 (m, 12H), 1.99–1.92 (m, 12H), 1.54–1.58 (m, 12H), 1.42–1.29 (m, 56H), 0.92–0.87 (m, 18H). ¹³C NMR (75 MHz, CDCl₃) δ: 150.10, 149.53, 149.30, 128.33, 126.72, 124.30, 124.17, 119.57, 107.98, 107.77, 107.06, 70.05, 69.68, 69.09, 32.17, 32.11, 29.91, 29.85, 29.73, 29.72, 29.61, 29.58, 29.39, 26.44, 26.39, 25.00, 22.94, 14.36. HRMS (MALDI) calcd. for C₇₄H₁₁₈O₆ *m/z*: 1102.8928; found: 1102.8924.

2,3,6,7-Tetrakis(decyloxy)-11,12-bis(hexyloxy)dibenz[a,c]anthracene (2g)

2,3-Bis[3,4-didecyloxyphenyl]-6,7-dihexyloxynaphthalene (0.90 g, 0.91 mmol) and FeCl₃ (0.88 g, 5.44 mmol) were used to obtain a light brown solid (0.85 g, 84.6% yield); mp 63 °C. ¹H NMR (300 MHz, CDCl₃) δ: 8.69 (s, 2H), 8.10 (s, 2H), 7.80 (s, 2H), 7.32 (s, 2H), 4.30–4.18 (m, 12H), 1.99–1.92 (m, 12H), 1.63–1.55 (m, 12H), 1.45–1.29 (m, 56H), 0.97–0.87 (m, 18H). ¹³C NMR (75 MHz, CDCl₃) δ: 150.12, 149.55, 149.32, 128.33, 126.72, 124.32, 124.19, 119.56, 108.04, 107.84, 107.09, 70.07, 69.69, 69.08, 32.16, 31.87, 29.93, 29.86, 29.78, 29.76, 29.61, 29.35, 26.44, 26.05, 22.93, 22.87, 14.33, 14.27. HRMS (MALDI) calcd. for C₇₄H₁₁₈O₆ *m/z*: 1102.8928; found: 1102.8923.

2,3,6,7-Tetrakis(decyloxy)-11,12-bis(octyloxy)dibenz[a,c]anthracene (2h)

2,3-Bis[3,4-didecyloxyphenyl]-6,7-dioctyloxynaphthalene (0.06 g, 0.052 mmol) and FeCl₃ (0.051 g, 0.315 mmol) were used to give a light brown solid (0.033 g, 55.1% yield); mp 64 °C. ¹H NMR (300 MHz, CDCl₃) δ: 8.70 (s, 2H), 8.11 (s, 2H), 7.80 (s, 2H), 7.32 (s, 2H), 4.28–4.20 (m, 12H), 1.97–1.94 (m, 12H), 1.59–1.55 (m, 12H), 1.36–1.25 (m, 64H), 0.90–0.86 (m, 18H). ¹³C NMR (75 MHz, CDCl₃) δ: 150.11, 149.54, 149.30, 128.33, 126.72, 124.31, 124.18, 119.57, 107.99, 107.77, 107.10, 70.04, 69.68, 69.08, 32.13, 32.02, 29.91, 29.4, 29.73, 29.71, 29.61, 29.51, 29.40, 26.44, 26.40, 24.98, 22.93, 14.30. HRMS (MALDI) calcd. for C₇₈H₁₂₆O₆ *m/z*: 1158.9554; found: 1158.9549.

2,3,6,7,11,12-Hexakis(decyloxy)dibenz[a,c]anthracene (2i)

2,3-Bis[3,4-didecyloxyphenyl]-6,7-didecyloxynaphthalene (1.214 g, 1.00 mmol) was dissolved in 20 mL dry CH₂Cl₂. FeCl₃ (0.97 g, 6.00 mmol) was added to the solution and stirred for 1 h, which yielded a light yellow solid (1.11 g, 91.4%); mp 60 °C. ¹H NMR (300 MHz, CDCl₃) δ: 8.69 (s, 2H), 8.10 (s, 2H), 7.80 (s, 2H), 7.32 (s, 2H), 4.28–4.20 (m, 12H), 1.97–1.95 (m, 12H), 1.59–1.55 (m, 12H), 1.43–1.28 (m, 72H), 0.91–0.87 (m, 18H). ¹³C NMR (75 MHz, CDCl₃) δ: 150.08, 149.50, 149.28, 128.31, 126.71, 124.29, 124.16, 119.55, 107.96, 107.74,

107.04, 70.03, 69.65, 69.07, 32.17, 29.94, 29.91, 29.87, 29.85, 29.79, 29.77, 29.72, 29.63, 29.39, 26.45, 26.39, 22.94, 14.35. HRMS (MALDI) calcd. for C₈₂H₁₃₄O₆ *m/z*: 1215.0180; found: 1215.0175.

General procedure for the dibromination of 2

The appropriate hexaalkoxydibenzanthracene 2 (1 equiv.) was dissolved in 50 mL chloroform. Bromine (2.3 equiv.) was added dropwise to the solution and the mixture was left to stir for 1 h. The reaction mixture was washed with sodium thiosulfate, water, and then brine. The organic layer was dried with Mg₂SO₄, filtered, and then dried. The crude product was purified using column chromatography with hexanes/dichloromethane (50:50). The product was then recrystallized in acetone to yield a light brown solid.

10,13-Dibromo-2,3,6,7,11,12-hexakis(hexyloxy)dibenz[a,c]anthracene (4a)

2,3,6,7,11,12-Hexakis(hexyloxy)dibenz[a,c]anthracene (0.067 g, 0.076 mmol) and Br₂ (0.028 g, 0.175 mmol) were used to yield a white solid (92% yield). ¹H NMR (300 MHz, CDCl₃) δ: 9.19 (s, 2H), 8.13 (s, 2H), 7.77 (s, 2H), 4.33–4.17 (m, 12H), 2.01–1.91 (m, 12H), 1.65–1.55 (m, 12H), 1.43–1.39 (m, 24H), 0.97–0.95 (m, 18H). ¹³C NMR (75 MHz, CDCl₃) δ: 150.42, 149.99, 149.39, 128.99, 129.09, 124.93, 123.34, 121.22, 116.17, 108.34, 107.59, 74.80, 69.90, 69.74, 31.96, 31.93, 30.55, 29.64, 29.61, 26.12, 26.08, 26.04, 22.93, 22.91, 22.90, 14.31, 14.28. HRMS (MALDI) calcd. for C₅₈H₈₄Br₂O₆ + H *m/z*: 878.6424; found: 878.6419.

10,13-Dibromo-2,3,6,7-tetrakis(hexyloxy)-11,12-bis(octyloxy)dibenz[a,c]anthracene (4b)

2,3,6,7-Tetrakis(hexyloxy)-11,12-bis(octyloxy)dibenz[a,c]anthracene (0.010 g, 0.106 mmol) and Br₂ (0.0374 g, 0.234 mmol) were used to obtain a light brown solid (0.082 g, 70.4% yield). ¹H NMR (300 MHz, CDCl₃) δ: 9.22 (s, 2H), 8.15 (s, 2H), 7.78 (s, 2H), 4.33–4.17 (m, 12H), 2.01–1.91 (m, 12H), 1.62–1.55 (m, 12H), 1.44–1.33 (m, 32H), 0.97–0.91 (m, 18H). ¹³C NMR (75 MHz, CDCl₃) δ: 150.44, 150.00, 149.41, 129.01, 128.12, 124.95, 123.36, 121.26, 116.19, 108.41, 107.61, 74.81, 69.91, 69.77, 32.11, 31.95, 31.92, 30.59, 29.74, 29.62, 29.59, 29.57, 26.39, 26.11, 26.08, 22.92, 22.90, 14.35, 14.31, 14.28. HRMS (MALDI) calcd. for C₆₂H₉₂Br₂O₆ + H *m/z*: 1090.5261; found: 1090.5220.

10,13-Dibromo-2,3,6,7-tetrakis(hexyloxy)-11,12-bis(decyloxy)dibenz[a,c]anthracene (4c)

2,3,6,7-Tetrakis(hexyloxy)-11,12-bis(decyloxy)dibenz[a,c]anthracene (0.07 g, 0.0705 mmol) and Br₂ (0.0248 g, 0.150 mmol) were used to obtain a light brown solid (0.071 g, 87.6% yield). ¹H NMR (300 MHz, CDCl₃) δ: 9.24 (s, 2H), 8.18 (s, 2H), 7.80 (s, 2H), 4.34–4.17 (m, 12H), 2.01–1.91 (m, 12H), 1.65–1.57 (m, 12H), 1.47–1.25 (m, 40H), 0.97–0.87 (m, 18H). ¹³C NMR (75 MHz, CDCl₃) δ: 150.49, 150.03, 149.46, 129.04, 128.15, 124.99, 123.40, 121.28, 116.19, 108.48, 107.65, 74.82, 69.93, 69.81, 32.15, 31.95, 31.91, 30.58, 29.90, 29.85, 29.77, 29.59, 26.38, 26.10, 26.07, 22.96, 22.91, 22.89, 14.34, 14.30, 14.27. HRMS (MALDI) calcd. for C₆₆H₁₀₀Br₂O₆ *m/z*: 1146.5887; found: 1146.5841.

10,13-Dibromo-2,3,6,7-tetrakis(octyloxy)-11,12-bis(hexyloxy)dibenz[a,c]anthracene (4d)

2,3,6,7-Tetrakis(octyloxy)-11,12-bis(hexyloxy)dibenz[a,c]anthracene (0.05 g, 0.05 mmol) and Br₂ (0.018 g, 0.11 mmol) were used to obtain a light brown solid (0.03 g, 52.2%). ¹H NMR (300 MHz, CDCl₃) δ: 9.21 (s, 2H), 8.15 (s, 2H), 7.77 (s, 2H), 4.32–4.17 (m, 12H), 2.00–1.91 (m, 12H), 1.61–1.29 (m, 52H), 0.94–0.89 (m, 18H). ¹³C NMR (75 MHz, CDCl₃) δ: 150.4, 150.0, 148.4, 129.0, 128.1, 124.9, 123.3, 121.2, 116.2, 108.4, 107.6, 74.8, 69.9, 69.8, 32.2, 31.9, 31.8, 30.5, 29.93, 29.86, 29.8, 29.7, 29.6, 26.45, 26.43, 26.0, 25.5, 22.9, 22.9, 14.33, 14.3.

10,13-Dibromo-2,3,6,7,11,12-hexakis(octyloxy)dibenz[a,c]anthracene (4e)

2,3,6,7,11,12-Hexakis(octyloxy)dibenz[a,c]anthracene (0.100 g, 0.095 mmol) and Br₂ (0.035 g, 0.219 mmol) were used to obtain a white solid (0.11 g, 96.1% yield). ¹H NMR (300 MHz, CDCl₃) δ: 9.12 (s, 2H), 8.07 (s, 2H), 7.72 (s, 2H), 4.31–4.18 (m, 12H), 2.01–1.92 (m, 12H), 1.65–1.57 (m, 12H), 1.43–1.33 (m, 48H), 0.94–0.89 (m, 18H). ¹³C NMR

(75 MHz, CDCl₃) δ: 149.51, 149.14, 148.49, 128.09, 127.20, 124.05, 122.45, 120.36, 115.38, 107.37, 106.64, 74.011, 69.04, 68.86, 31.35, 29.86, 29.01, 28.94, 28.90, 28.85, 25.70, 25.68, 25.66, 22.17, 13.58. HRMS (MALDI) calcd. for C₇₀H₁₀₈Br₂O₆ *m/z*: 1202.6513; found: 1202.6544.

10,13-Dibromo-2,3,6,7-tetrakis(octyloxy)-11,12-bis(decyloxy)dibenz[a,c]anthracene (14f)

2,3,6,7-Tetrakis(octyloxy)-11,12-bis(decyloxy)dibenz[a,c]anthracene (0.100 g, 0.091 mmol) and Br₂ (0.033 g, 0.208 mmol) were used to obtain a white solid (0.097 g, 84.9% yield). ¹H NMR (300 MHz, CDCl₃) δ: 9.16 (s, 2H), 8.10 (s, 2H), 7.75 (s, 2H), 4.32–4.17 (m, 12H), 2.01–1.92 (m, 12H), 1.62–1.57 (m, 12H), 1.43–1.30 (m, 56H), 0.93–0.88 (m, 18H). ¹³C NMR (75 MHz, CDCl₃) δ: 150.31, 149.93, 149.26, 128.90, 128.00, 124.84, 123.25, 121.15, 116.17, 108.17, 107.44, 74.79, 69.84, 69.66, 32.18, 32.13, 32.12, 30.63, 29.95, 29.90, 29.82, 29.79, 29.77, 29.71, 29.67, 29.63, 29.14, 26.48, 26.46, 26.43, 22.96, 14.36. HRMS (MALDI) calcd. for C₇₄H₁₁₆Br₂O₆ *m/z*: 1258.7139; found: 1258.7079.

10,13-Dibromo-2,3,6,7-tetrakis(decyloxy)-11,12-bis(hexyloxy)dibenz[a,c]anthracene (14g)

2,3,6,7-Tetrakis(decyloxy)-11,12-bis(hexyloxy)dibenz[a,c]anthracene (0.100 g, 0.091 mmol) and Br₂ (0.033 g, 0.209 mmol) were used to obtain a light brown solid (0.101 g, 88.0% yield). ¹H NMR (300 MHz, CDCl₃) δ: 9.24 (s, 2H), 8.17 (s, 2H), 7.79 (s, 2H), 4.33–4.17 (m, 12H), 2.01–1.92 (m, 12H), 1.64–1.59 (m, 12H), 1.44–1.29 (m, 56H), 0.93–0.87 (m, 18H). ¹³C NMR (75 MHz, CDCl₃) δ: 150.46, 150.01, 149.43, 129.03, 128.13, 124.98, 123.38, 121.28, 116.19, 108.48, 107.68, 74.83, 69.94, 69.80, 32.17, 31.95, 30.55, 29.96, 29.94, 29.87, 29.79, 29.69, 29.62, 26.46, 26.43, 26.04, 22.94, 22.91, 14.35, 14.32. HRMS (MALDI) calcd. for C₇₄H₁₁₆Br₂O₆ *m/z*: 11258.7139; found: 1258.7156.

10,13-Dibromo-2,3,6,7-tetrakis(decyloxy)-11,12-bis(octyloxy)dibenz[a,c]anthracene (14h)

2,3,6,7-Tetrakis(decyloxy)-11,12-bis(octyloxy)dibenz[a,c]anthracene (0.010 g, 0.0086 mmol) and Br₂ (0.0032 g, 0.0198 mmol) were used to obtain a white solid (0.0107 g, 94.0% yield). ¹H (300 MHz, CDCl₃) δ: 9.24 (s, 2H), 8.18 (s, 2H), 7.79 (s, 2H), 4.33–4.17 (m, 12H), 2.01–1.91 (m, 12H), 1.60–1.55 (m, 12H), 1.43–1.25 (m, 64H), 0.91–0.86 (m, 18H). ¹³C NMR (75 MHz, CDCl₃) δ: 150.48, 150.03, 149.44, 129.03, 128.15, 124.99, 123.38, 121.29, 116.19, 108.51, 107.68, 74.83, 69.93, 69.81, 32.16, 32.10, 30.57, 29.93, 29.86, 29.77, 29.72, 29.61, 29.55, 26.43, 26.38, 25.70, 22.92, 14.34. HRMS (MALDI) calcd. for C₇₈H₁₂₄Br₂O₆ *m/z*: 1314.7765; found: 1314.7744.

10,13-Dibromo-2,3,6,7,11,12-hexakis(decyloxy)dibenz[a,c]anthracene (4i)¹⁹

2,3,6,7,11,12-Hexakis(decyloxy)dibenz[a,c]anthracene (0.300 g, 0.247 mmol) and Br₂ (0.029 mL, 0.567 mmol) were used to give a light brown solid (0.319 g, 94.0% yield). ¹H NMR (300 MHz, CDCl₃) δ: 9.25 (s, 2H), 8.18 (s, 2H), 7.79 (s, 2H), 4.32 (t, *J* = 6.60 Hz, 4H), 4.43 (t, *J* = 6.30 Hz), 4.18 (t, *J* = 6.30 Hz, 4H), 2.00–1.91 (m, 12H), 1.60–1.54 (m, 12H), 1.38–1.26 (m, 72H), 0.90–0.86 (m, 18H). ¹³C NMR (75 MHz, CDCl₃) δ: 150.47, 150.02, 149.43, 129.04, 128.14, 124.98, 123.39, 121.29, 116.20, 108.34, 107.67, 74.83, 69.94, 69.80, 32.17, 30.59, 29.95, 29.93, 29.91, 29.87, 29.78, 29.62, 29.60, 26.43, 26.39, 25.00, 22.94, 14.34. HRMS (MALDI) calcd. for C₈₂H₁₃₂Br₂O₆ + H *m/z*: 1370.8391; found: 1370.8385.

Synthesis of 10-bromo-2,3,6,7,11,12-hexakis(decyloxy)dibenz[a,c]anthracene (6)¹⁹

2,3,6,7,11,12-Hexakis(decyloxy)dibenz[a,c]anthracene (0.250 g, 0.206 mmol) was dissolved in 50 mL CHCl₃. Bromine (0.035 g, 0.216 mmol) was added dropwise to the solution and left to stir for 1 h. The organic layer was washed with sodium thiosulfate, water, and then brine. The organic layer was dried with MgSO₄, filtered, and the solvent was removed under reduced pressure. Column chromatography was performed on the crude product with hexanes/DCM (50:50), followed by recrystallization in acetone to yield a pale yellow-brown solid (0.243 g, 91.1% yield). ¹H NMR (300 MHz,

CDCl₃, 30 mmol/L) δ: 9.15 (s, 1H), 8.65 (s, 1H), 8.17 (s, 1H), 8.07 (s, 1H), 7.78 (s, 2H), 7.30 (s, 1H), 4.31–4.22 (m, 8H), 4.18–4.16 (m, 4H), 1.98–1.91 (m, 12H), 1.60–1.56 (m, 12H), 1.42–1.29 (m, 84H), 0.91–0.87 (m, 18H). ¹³C NMR (75 MHz, CDCl₃) δ: 152.29, 149.98, 149.87, 149.36, 149.26, 147.17, 129.89, 128.14, 127.36, 126.51, 124.73, 124.30, 124.16, 123.48, 120.69, 119.96, 116.28, 108.15, 107.96, 107.81, 107.70, 106.84, 73.94, 69.99, 69.92, 69.69, 68.93, 32.18, 30.63, 29.96, 29.92, 29.89, 29.81, 29.74, 29.64, 29.53, 26.53, 26.46, 22.95, 14.36. HRMS (MALDI) calcd. for C₈₂H₁₃₃BrO₆ + H *m/z*: 1292.9286; found: 1292.9280.

Synthesis of 10-cyano-2,3,6,7,11,12-hexakis(decyloxy)dibenz[a,c]anthracene (7)¹⁹

10-Bromo-2,3,6,7,11,12-hexakis(decyloxy)dibenz[a,c]anthracene (0.10 g, 0.077 mmol) was dissolved in dry dimethylformamide (DMF; 5 mL). CuCN (9.0 mg, 0.10 mmol) was added to the solution. The reaction was fitted with a condenser and heated to reflux for 18 h while kept under a N₂ atmosphere. The solution was cooled to room temperature, followed by the addition of 20 mL of water. Ethylenediamine (1 mL) was added to the solution and shaken. It was then extracted with DCM (3 × 25 mL), and washed with water followed by 1 mol/L HCl. The organic layer was dried with MgSO₄, filtered, and the solvent was removed under reduced pressure. A brown solid crude product was obtained. Column chromatography was performed with hexanes/dichloromethane (50:50), followed by recrystallization in acetone to yield a bright yellow solid (0.042 g, 48% yield). ¹H NMR (300 MHz, CDCl₃) δ: 8.73 (s, 1H), 8.37 (s, 1H), 7.94 (s, 1H), 7.80 (s, 1H), 7.63 (s, 1H), 7.62 (s, 1H), 7.28 (s, 1H), 4.34 (t, *J* = 6.6 Hz, 2H), 4.30–4.22 (m, 8H), 4.17 (t, *J* = 6.3 Hz, 2H), 1.96–1.91 (m, 12H), 1.56–1.52 (m, 12H), 1.43–1.26 (m, 72H), 0.93–0.89 (m, 18H). ¹³C NMR (75 MHz, CDCl₃) δ: 154.90, 150.62, 150.08, 150.00, 149.44, 149.14, 128.38, 128.35, 128.13, 125.76, 124.57, 124.37, 123.40, 123.04, 120.10, 117.59, 116.11, 112.17, 107.66, 107.52, 107.45, 107.28, 101.80, 75.36, 69.89, 69.72, 69.58, 69.10, 32.21, 32.20, 30.61, 30.01, 29.99, 29.93, 29.89, 29.80, 29.76, 29.68, 29.65, 29.48, 26.52, 26.19, 22.97, 14.37. HRMS (MALDI) calcd. for C₈₃H₁₃₃NO₆ + H *m/z*: 1240.0133; found: 1240.0127.

Synthesis of 10-iodo-2,3,6,7,11,12-hexakis(decyloxy)dibenz[a,c]anthracene (8)

10-Bromo-2,3,6,7,11,12-hexakis(decyloxy)dibenz[a,c]anthracene (6; 0.247 g, 0.191 mmol) was added to 25 mL dry THF. The solution was placed in an ice bath and cooled to –42 °C. To the cooled solution was added *n*-BuLi (0.11 mL, 2.10 mol/L, 1.2 equiv.) where it was stirred for 30 min while maintaining –42 °C. Molecular iodine (0.097 g, 0.382 mmol) was added to solution, and then it was allowed to warm to room temperature. The mixture was then treated with saturated sodium thiosulfate (50 mL). The organic layer was removed and further washed with brine (1 × 50 mL) and H₂O (1 × 50 mL). It was dried with MgSO₄ and the solvent was removed under reduced pressure. Column chromatography was performed with hexanes/DCM (70:30). The product was recrystallized in acetone to yield a white solid (0.130 g, 50.7% yield). ¹H NMR (300 MHz, CDCl₃) δ: 9.12 (s, 1H), 8.65 (s, 1H), 8.21 (s, 1H), 8.10 (s, 1H), 7.80 (s, 2H), 7.34 (s, 1H), 4.32–4.15 (m, 12H), 1.95–1.93 (m, 12H), 1.60–1.54 (m, 12H), 1.42–1.29 (m, 72H), 0.91–0.86 (m, 18H). ¹³C NMR (75 MHz, CDCl₃) δ: 151.50, 150.28, 149.99, 149.85, 149.38, 149.29, 129.98, 128.71, 128.08, 127.73, 125.97, 124.74, 124.25, 124.09, 123.44, 120.02, 108.08, 108.03, 107.91, 107.77, 96.18, 73.75, 70.05, 69.94, 69.72, 69.63, 68.89, 53.63, 32.16, 30.65, 29.94, 29.91, 29.86, 29.78, 29.73, 29.62, 29.54, 26.53, 26.48, 26.44, 25.01, 22.93, 14.34.

Synthesis of 10,13-dicyano-2,3,6,7,11,12-hexakis(decyloxy)dibenz[a,c]anthracene (5)¹⁹

10,13-Dibromo-2,3,6,7,11,12-hexakis(decyloxy)dibenz[a,c]anthracene (0.42 g, 0.306 mmol) was dissolved in 10 mL dry DMF. CuCN (69 mg, 0.76 mmol) was added to the solution. The reaction was heated to reflux and stirred for 24 h under a N₂ atmosphere. The solution was then cooled to room temperature; 10 mL of ethyl-

enediamine was added, followed by 20 mL H₂O. It was then extracted with DCM (3 × 20 mL). The organic layer was washed with 1 mol/L HCl (3 × 50 mL), H₂O (50 mL), and brine (50 mL). The organic layer was dried with MgSO₄, filtered, and concentrated under reduced pressure. Column chromatography was performed with hexanes/dichloromethane (60:40), followed by recrystallization in acetone to yield a bright orange solid (0.04 g, 10.3% yield). ¹H NMR (300 MHz, CDCl₃) δ: 8.63 (s, 2H), 7.71 (s, 2H), 7.58 (s, 2H), 4.44 (t, *J* = 6.9 Hz, 4H), 4.21 (m, 8H), 1.96 (m, 12H), 1.61 (m, 12H), 1.29 (m, 72H), 0.89 (m, 18H). ¹³C NMR (75 MHz, CDCl₃) δ: 155.71, 150.55, 149.14, 129.72, 126.17, 124.72, 122.01, 118.29, 114.95, 107.02, 106.72, 106.50, 76.31, 69.50, 69.30, 32.19, 30.57, 30.04, 30.00, 29.97, 29.96, 29.94, 29.78, 29.75, 29.72, 29.66, 29.64, 26.50, 26.18, 22.94, 14.35. HRMS (MALDI) calcd. for C₈₃H₁₃₃NO₆ + H *m/z*: 1265.0085; found: 1265.0080.

Synthesis of 2,3-dibromo-5-nitro-6,7-bis(decyloxy)naphthalene (16)

Nitric acid (50 mL) was cooled to 0 °C in an ice bath, where 20 drops of concentrated sulfuric acid were added. 2,3-Dibromo-6,7-bis(decyloxy)naphthalene (2.00 g, 3.34 mmol) was slowly added to the acidic mixture. The solution was stirred vigorously overnight while allowing the mixture to warm to room temperature overnight (12 h). The solution was neutralized with saturated NaHCO₃ (50 mL). The product was then extracted with 50 mL EtOAc, followed by a washing with NaHCO₃ (1 × 50 mL), brine (50 mL), and water (50 mL). The organic layer was dried with MgSO₄, filtered, and concentrated under reduced pressure. Column chromatography was performed with hexanes/EtOAc (90:10), followed by a recrystallization in EtOH to give a white solid (1.18 g, 54.9% yield). ¹H NMR (300 MHz, CDCl₃) δ: 8.01 (s, 1H), 7.87 (s, 1H), 7.10 (s, 1H), 4.21 (t, *J* = 6.6 Hz, 2H), 4.10 (t, *J* = 6.3 Hz, 2H), 1.92–1.87 (m, 2H), 1.79–1.75 (m, 2H), 1.29–1.25 (m, 28H), 0.90–0.86 (m, 6H). ¹³C NMR (75 MHz, CDCl₃) δ: 152.50, 142.58, 140.90, 130.98, 129.95, 125.64, 123.14, 122.51, 120.22, 108.81, 75.69, 69.61, 32.12, 30.19, 29.81, 29.78, 29.61, 29.55, 29.22, 26.36, 25.92, 22.91, 14.32.

Synthesis of 2,3-bis[3,4-didecyloxyphenyl]-6,7-didecyloxy-5-nitronaphthalene (17)

A flask was charged with 2,3-dibromo-5-nitro-6,7-bis(decyloxy)naphthalene (1.00 g, 1.55 mmol), 1-pinacolatoboron-3,4-bis(decyloxy)benzene (1.67 g, 3.24 mmol), Pd(OAc)₂ (0.035 g, 0.16 mmol), and triphenylphosphine (0.081 g, 0.31 mmol). A 15 mL degassed toluene to reagent mixture was added. The organic solution was combined with 7 mL of 2 mol/L K₃PO₄. The reaction was fitted with a condenser, heated to 80 °C, and left to stir for 48 h under a N₂ atmosphere. The reaction mixture was cooled to room temperature, and dichloromethane (20 mL) was added. The organic layer was separated and washed with water and then brine. The organic layer was dried with MgSO₄, filtered, and the solvent was removed under reduced pressure. Column chromatography was performed with hexanes/dichloromethane (60:40), followed by recrystallization in acetone to yield a yellow solid (1.15 g, 58.9% yield). ¹H NMR (300 MHz, CDCl₃) δ: 7.74 (s, 1H), 7.60 (s, 1H), 7.27 (s, 1H), 6.79 (s, 4H), 6.63 (s, 1H), 6.59 (s, 1H), 4.23 (t, *J* = 6.6 Hz, 2H), 4.14 (t, *J* = 6.7 Hz, 2H), 3.97 (t, *J* = 6.6 Hz, 4H), 3.70–3.67 (m, 4H), 1.91–1.79 (m, 12H), 1.68–1.64 (m, 4H), 1.49–1.45 (m, 8H), 1.30–1.27 (m, 72H), 0.91–0.87 (m, 18H). ¹³C NMR (75 MHz, CDCl₃) δ: 151.3, 148.5, 141.9, 141.2, 139.8, 139.5, 133.7, 133.6, 129.4, 119.4, 116.2, 115.8, 75.3, 69.3, 69.2, 31.97, 31.95, 31.93, 30.05, 29.7, 29.68, 29.66, 29.64, 29.60, 29.52, 29.47, 29.43, 29.39, 29.38, 29.36, 29.2, 26.2, 26.11, 26.10, 26.06, 25.8, 22.7, 14.1. HRMS (MALDI) calcd. for C₈₂H₁₃₅NO₈ + H *m/z*: 1262.0188; found: 1262.0182.

Synthesis of 10-nitro-2,3,6,7,11,12-hexakis(decyloxy)dibenz[a,c]anthracene (9)

2,3-Bis[3,4-didecyloxyphenyl]-6,7-didecyloxy-5-nitronaphthalene (0.500 g, 0.396 mmol) was added to 20 mL of dry dichloromethane.

FeCl₃ (0.385 g, 2.38 mmol) was added to the solution, placed under a N₂ atmosphere, and left to stir for 1 h. The mixture was poured into MeOH (150 mL) and placed in a freezer for 1 h. A suction filtration was performed on the resulting precipitate, and then washed with cold MeOH. A short flash column chromatography was done with dichloromethane to remove the excess FeCl₃, followed by recrystallization in acetone to yield a yellow solid (0.453 g, 90.7% yield). ¹H NMR (300 MHz, CDCl₃) δ: 8.48 (s, 1H), 8.37 (s, 1H), 7.91 (s, 1H), 7.74 (s, 1H), 7.63 (s, 1H), 7.61 (s, 1H), 7.25 (s, 1H), 4.27–4.14 (m, 12H), 1.99–1.95 (m, 10H), 1.86–1.81 (m, 2H), 1.59–1.54 (m, 12H), 1.30–1.25 (m, 72H), 0.91–0.86 (m, 18H). ¹³C NMR (75 MHz, CDCl₃) δ: 150.78, 150.09, 149.99, 149.36, 149.13, 141.64, 141.60, 128.50, 128.30, 128.07, 124.68, 124.32, 123.29, 122.87, 119.85, 118.29, 114.11, 109.38, 107.60, 107.48, 107.41, 107.15, 75.57, 69.90, 69.63, 69.57, 69.49, 69.25, 32.22, 32.21, 32.19, 30.37, 30.01, 29.95, 29.93, 29.91, 29.88, 29.83, 29.79, 29.76, 29.68, 29.65, 29.51, 26.55, 26.51, 26.10, 22.97, 14.37. HRMS (MALDI) calcd. for C₈₂H₁₃₃NO₈ + H *m/z*: 1260.0031; found: 1260.0026.

Synthesis of 10-amino-2,3,6,7,11,12-hexakis(decyloxy)dibenz[a,c]anthracene (10)

10-Nitro-2,3,6,7,11,12-hexakis(decyloxy)dibenz[a,c]anthracene (0.453 g, 0.359 mmol) and NiCl₂·6H₂O (0.426 g, 1.795 mmol) were dissolved in 20 mL dry THF and 7 mL dry MeOH. The solution was an orange-green colour. NaBH₄ was added in small portions to the solution, where the mixture turned black. Stirring was continued for 45 min after the addition of the base. The crude mixture was filtered and washed with dichloromethane. It was then dissolved in 50 mL of dichloromethane. The organic layer was washed with water (50 mL) and brine (50 mL). The organic layer was dried with MgSO₄, filtered, and the solvent was removed under reduced pressure. Column chromatography was performed with hexanes/dichloromethane (60:40 → 40:60), followed by recrystallization in acetone to give a light brown solid (0.108 g, 24.4% yield). ¹H NMR (300 MHz, CDCl₃) δ: 8.72 (s, 1H), 8.66 (s, 1H), 8.11 (s, 1H), 8.08 (s, 1H), 7.78 (s, 2H), 6.91 (s, 1H), 4.48 (bs, 2H), 4.29–4.21 (m, 8H), 4.17 (t, *J* = 6.6 Hz, 2H), 4.11 (t, *J* = 6.6 Hz, 2H), 1.99–1.85 (m, 12H), 1.59–1.55 (m, 12H), 1.49–1.21 (m, 72H), 0.89 (t, *J* = 6.6 Hz, 18H). ¹³C NMR (75 MHz, CDCl₃) δ: 152.58, 149.69, 149.59, 149.29, 149.26, 134.51, 133.68, 129.95, 127.71, 125.51, 124.46, 124.44, 124.23, 124.03, 120.23, 120.00, 114.51, 108.07, 107.92, 107.85, 107.80, 98.20, 73.43, 69.99, 69.62, 68.39, 32.18, 30.81, 29.95, 29.88, 29.80, 29.72, 29.64, 29.62, 26.58, 26.51, 26.46, 26.44, 22.95, 14.36. HRMS (MALDI) calcd. for C₈₂H₁₃₅NO₆ + H *m/z*: 1230.0289; found: 1230.0284.

Mesophase characterization

Polarized optical microscopy studies were carried out using an Olympus BX-51 polarized optical microscope equipped with a Linkam LTS 350 heating stage and a digital camera. Differential scanning calorimetry (DSC) studies were carried out using a TA Instruments DSC Q200 with a scanning rate of 5 °C/min.

Acknowledgement

We are grateful to the Natural Sciences and Engineering Research Council of Canada, the American Chemical Society (ACS) Petroleum Research Fund, the Canada Foundation for Innovation, the Ontario Research Fund, the Ontario Early Researcher Award, and Wilfrid Laurier University for financial support. This work was also supported by the Research Support Fund. We also thank Dr. A. Furtos at the Université de Montréal for mass spectrometric analyses.

References

- (1) Kumar, S. *Chemistry of Discotic Liquid Crystals*; CRC Press: Boca Raton, 2011.
- (2) Kumar, S. In *Handbook of Liquid Crystals*; Goodby, J. W., Ed.; Wiley VCH: 2014; Vol. 4, p. 467.
- (3) Kumar, S. *Chem. Soc. Rev.* **2006**, *35*, 83. doi:10.1039/B506619K.
- (4) Laschat, S.; Baro, A.; Steinke, N.; Giesselmann, F.; Hagele, C.; Scalia, G.;

- Judele, R.; Kapatsina, E.; Sauer, S.; Schreivogel, A.; Tosoni, M. *Angew. Chem. Int. Ed. Engl.* **2007**, *46*, 4832. doi:10.1002/anie.200604203.
- (5) Wohrle, T.; Wurzbach, I.; Kirres, J.; Kostidou, A.; Kapernaum, N.; Litterscheidt, J.; Haenle, J. C.; Staffeld, P.; Baro, A.; Giesselmann, F.; Laschat, S. *Chem. Rev.* **2016**, *116*, 1139. doi:10.1021/acs.chemrev.5b00190.
- (6) Sergeev, S.; Pisula, W.; Geerts, Y. H. *Chem. Soc. Rev.* **2007**, *36*, 1902. doi:10.1039/b417320c.
- (7) Muller, G. R. J.; Meiners, C.; Enkelmann, V.; Geerts, Y.; Mullen, K. J. *Mater. Chem.* **1998**, *8*, 61. doi:10.1039/A705910H.
- (8) Msayib, K.; Makhseed, S.; McKeown, N. B. J. *Mater. Chem.* **2001**, *11*, 2784. doi:10.1039/B103145G.
- (9) Pisula, W.; Tomovic, Z.; Simpson, C.; Kastler, M.; Pakula, T.; Mullen, K. *Chem. Mater.* **2005**, *17*, 4296. doi:10.1021/cm050251c.
- (10) Herwig, P.; Kayser, C. W.; Mullen, K.; Spiess, H. W. *Adv. Mater.* **1996**, *8*, 510. doi:10.1002/adma.19960080613.
- (11) Lau, K.; Foster, J.; Williams, V. *Chem. Commun.* **2003**, 2172. doi:10.1039/B305462D.
- (12) Yatabe, T.; Harbison, M. A.; Brand, J. D.; Wagner, M.; Mullen, K.; Samori, P.; Rabe, J. P. J. *Mater. Chem.* **2000**, *10*, 1519. doi:10.1039/B001162M.
- (13) Foster, E. J.; Jones, R. B.; Lavigueur, C.; Williams, V. E. *J. Am. Chem. Soc.* **2006**, *128*, 8569. doi:10.1021/ja0613198.
- (14) Boden, N.; Bushby, R. J.; Cammidge, A. N.; Duckworth, S.; Headdock, G. *J. Mater. Chem.* **1997**, *7*, 601. doi:10.1039/A606447G.
- (15) Boden, N.; Bushby, R. J.; Lu, Z. B.; Cammidge, A. N. *Liq. Cryst.* **1999**, *26*, 495. doi:10.1080/026782999204930.
- (16) Boden, N.; Movaghar, B. In *Handbook of Liquid Crystals*; Demus, D., Goodby, J., Gray, G. W., Spiess, H.-W., Vill, V., Eds.; Wiley-VCH: New York; Vol. 2B, p. 781.
- (17) Boden, N.; Borner, R. C.; Bushby, R. J.; Cammidge, A. N.; Jesudason, M. V. *Liq. Cryst.* **1993**, *15*, 851. doi:10.1080/02678299308036504.
- (18) Kumar, S. *Liq. Cryst.* **2004**, *31*, 1037. doi:10.1080/02678290410001724746.
- (19) Paquette, J. A.; Yardley, C. J.; Psutka, K. M.; Cochran, M. A.; Calderon, O.; Williams, V. E.; Maly, K. E. *Chem. Commun.* **2012**, *48*, 8210. doi:10.1039/C2CC33407K.
- (20) Psutka, K. M.; Bozek, K. J. A.; Maly, K. E. *Org. Lett.* **2014**, *16*, 5442. doi:10.1021/ol502678m.
- (21) Psutka, K. M.; Williams, J.; Paquette, J. A.; Calderon, O.; Bozek, K. J. A.; Williams, V. E.; Maly, K. E. *Eur. J. Org. Chem.* **2015**, 1456. doi:10.1002/ejoc.201403504.
- (22) Cozzi, F.; Cinquini, M.; Annunziata, R.; Siegel, J. S. *J. Am. Chem. Soc.* **1993**, *115*, 5330. doi:10.1021/ja00065a069.
- (23) Cozzi, F.; Ponzini, F.; Annunziata, R.; Cinquini, M.; Siegel, J. S. *Angew. Chem. Int. Ed.* **1995**, *34*, 1019. doi:10.1002/anie.199510191.
- (24) Cammidge, A. N.; Chausson, C.; Gopee, H.; Li, J. J.; Hughes, D. L. *Chem. Commun.* **2009**, 7375. doi:10.1039/B913678A.
- (25) Chen, Z. H.; Swager, T. M. *Org. Lett.* **2007**, *9*, 997. doi:10.1021/ol062999m.
- (26) Lynett, P. T.; Maly, K. E. *Org. Lett.* **2009**, *11*, 3726. doi:10.1021/ol9013443.
- (27) Kumar, S.; Manickam, M.; Balagurusamy, V. S. K.; Schonherr, H. *Liq. Cryst.* **1999**, *26*, 1455. doi:10.1080/026782999203788.
- (28) Cross, S. J.; Goodby, J. W.; Hall, A. W.; Hird, M.; Kelly, S. M.; Toyne, K. J.; Wu, C. *Liq. Cryst.* **1998**, *25*, 1. doi:10.1080/026782998206443.
- (29) Destrade, C.; Tinh, N. H.; Gasparoux, H.; Malthete, J.; Levelut, A. M. *Mol. Cryst. Liq. Cryst.* **1981**, *71*, 111. doi:10.1080/00268948108072721.
- (30) Maly, K. E. *Cryst. Growth Des.* **2011**, *11*, 5628. doi:10.1021/cg201182p.
- (31) Cammidge, A. N. *Philos. Trans. A Math. Phys. Eng. Sci.* **2006**, *364*, 2697. doi:10.1098/rsta.2006.1847.
- (32) Boden, N.; Bushby, R. J.; Cammidge, A. N.; Headdock, G. *J. Mater. Chem.* **1995**, *5*, 2275. doi:10.1039/JM950502275.
- (33) Kumar, S.; Manickam, M. *Mol. Cryst. Liq. Cryst.* **1998**, *309*, 291. doi:10.1080/10587259808045535.